Available online at www.sciencedirect.com
SCIENCE DIRECT
Journal of Power Sources 145 (2005) 572–581
JOURNAL OF POWER SOURCES
www.elsevier.com/locate/jpowsour

Three-dimensional analysis for effect of channel configuration on the performance of a small air-breathing proton exchange membrane fuel cell (PEMFC)

Wang Ying [a,b], Tae-Hyun Yang [b], Won-Yong Lee [b,*], J. Ke [a], Chang-Soo Kim [b]

[a] *Mechanical Engineering School, Southwest Jiaotong University, Chengdu, 610031 Sichuan, PR China*
[b] *Fuel Cell Research Center, Korea Institute of Energy Research, P.O. Box 103, Yusong, Daejeon 305-343, South Korea*

Accepted 7 February 2005
Available online 23 May 2005

Abstract

A coupled 3D mathematical model for the real geometry of an air-breathing proton exchange membrane (PEMFC) was developed and validated by experimental data. The free convection in the cathode side was included in the model. The concentration over-potential was considered as a function of mass transfer coefficient of oxygen in the catalyst layer. Governing equations possess the features that fluid dynamics, mass/heat transfer are coupled with the electrochemical reactions. The model was solved in a commercial software STAR-CD based on the finite-difference and finite-volume methods, and the electrochemical features and water transport in membrane are solved simultaneously through a user-specific subroutine. To investigate the effect of channel configuration on air-breathing fuel cell performance, calculations for three different widths of channels have been executed. Results show the best performance can be obtained in the cell with cathode channel width of 3 mm (open ratio of 75.9%).

Keywords: Free convection; Air-breathing; PEMFC; Channel width; Open ratio

1. Introduction

The air-breathing proton exchange membrane fuel cell (PEMFC) that operates at ambient temperature without humidifier and air compressor is one of the candidates for small fuel cells, which are the most interesting alternatives for power production in portable applications. A schematic structure of an air-breathing PEMFC used in our libratory is illustrated in Fig. 1. This single air-breathing PEMFC consists of seven components. The electrolyte used here is Nafion 112 cation exchange membrane with a perfluorinated polysulfonate structure developed by Du Pont, and two electrodes are made of carbon-supported platinum catalyst. These three parts are assembled into a sandwich structure to form a membrane-electrode-assembly (MEA). The teflonated porous carbon paper is selected as gas diffusion backing. The cathode bipolar plate is machined into straight channel, and anode plate is designed as serpentine groove as shown in Fig. 1. The bipolar plates produce a gas way for cathode and anode reactant transport into the cell, and play also a significant role on the characteristics of membrane hydration. These aspects greatly influence system efficiency either for forced air suppling PEMFCs or air-breathing PEMFCs. For the air-breathing PEMFCs, the air is induced into the cathode channel by free convection. When the air-breathing PEMFC is working, the heat is transferred from irreversibility losses. The heated fluid becomes less dense and flows upwards, while packets of cooled fluid become denser and sink. Meanwhile the density of air is also changed by the oxygen consumption and the water product in electrochemical reaction. And thus natural convection appears and oxygen breathes into the cathode by buoyancy

* Corresponding author. Tel.: +82 42 860 3506; fax: +82 42 860 3739.
E-mail addresses: wy82lee@kier.re.kr, wangying@kier.re.kr (W.-Y. Lee).

0378-7753/$ – see front matter © 2005 Elsevier B.V. All rights reserved.
doi:10.1016/j.jpowsour.2005.02.066

Nomenclature

A_{CV}	specific area for control volume ($m^2\,m^{-3}$)
B	coefficient in concentration over-potential equation (3.4×10^{-4})
C	molar concentration ($mol\,cm^{-3}$)
D	mass diffusion coefficient ($cm^2\,s^{-1}$)
F	Faraday's constant (96,487 $C\,mol^{-1}$)
g	gravity ($m\,s^{-2}$)
h_M	mass transfer coefficient ($m\,s^{-1}$)
I	local current density ($A\,cm^{-2}$)
I_{lim}	concentration limiting current density ($A\,cm^{-2}$)
I^0	exchange current density ($A\,cm^{-2}$)
k_P	hydraulic permeability (cm^2)
L	characteristic length (m)
$\dot{m}_{O_2}$	oxygen mass flux ($kg\,m^{-2}\,s^{-1}$)
M	molar mass of gases ($kg\,mol^{-1}$)
n_d	electro-osmotic drag coefficient
R	gas constant ($8.314\,J\,mol^{-1}\,K^{-1}$)
S	source term in governing equation
Sh	Sherwood number
t_m	membrane thickness (cm)
T	temperature (K)
$\vec{u}$	velocity ($m\,s^{-1}$)
V_C	cell voltage (V)
V_{OC}	open circuit voltage (V)
w	width (cm)
X	mass fraction (0–1.0)

Greek letters

α	net water transfer coefficient per proton
ε	porosity
η	over-potential (V)
ι	land area fraction
λ	water contents of membrane
μ	dynamic viscosity ($kg\,m^{-3}$)
$\overline{o}$	open ratio of air channel (%)
ρ	density ($kg\,m^{-3}$)
σ_m	membrane conductivity ($S\,cm^{-1}$)
∇	change in . . .

Indices

a	anode
act	activation
c	cathode
channel	channel
conc	concentration
H_2	hydrogen
i	species
ohm	ohmic losses
O_2	oxygen
m	membrane
mix	gas mixture
M	mass
rib	rib
sat	saturated
total	total activity area
u	momentum source
w	water
∞	in quiescence air

forces. Concentration gradient and temperature difference are the driving force of natural convection, the first one is so-called mass transfer driven natural convection, the last one is called heat transfer driven natural convection. The density difference is approximately proportional to the temperature difference and concentration gradient of oxygen. If there is not enough air supplied to channel because of weak natural convection or liquid water blocking in the gas way, the oxygen in the catalyst layer cannot be replenished. Hence the performance of the cell is diminished extremely due to oxygen transport limitation losses. If the oxygen concentration is reduced to some extent in the catalyst layer, the cell will stop working. The current density at which the oxygen is used up is called the limitation current density. The cell cannot work beyond the limitation current density. Several literatures have contributed to the studying of the performance of air-breathing PEMFC [1–5]. It shows the performance drop caused by oxygen mass limitation losses is very serious in air-breathing PEMFCs. One will not achieve a better performance for an air-breathing PEMFC by simply using the design rule for a typical PEMFC with a forced convection air channel. Rather, one must redesign each component of the fuel cell considering the special issues caused by the way of air supply in the cathode side. In the case of the cathode channel design, the channel configuration is generally complex and narrow in the typical forced convection air supply PEMFCs in order to achieve a practical pressure drop to drive out unwanted water and distribute gas in every cell and every section of channel uniformly. The serpentine flow field is frequently used in forced convection PEMFCs. The

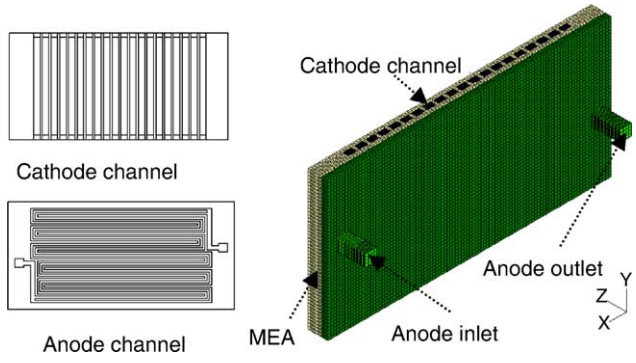

Fig. 1. Scheme of channel configuration and geometry of an air-breathing PEMFC.

pressure drop is the most important parameter to scale the channel configuration in a typical PEMFC. However, in an air-breathing PEMFC with a vertical air channel, the channel configuration could be relatively simple and wide to induce more oxygen into the channel and strengthen mass and heat transfer. The mass transfer rate is vital parameter for designing the air channel. To optimize the channel configuration and to improve the performance, it is necessary to build an integrated mathematical model and to perform a numerical calculation for an air-breathing PEMFC.

Over the past few years researchers have placed emphasis on the three-dimensional (3D) mode to accurately predict the performance of fuel cells. Dutta et al. [5] reported a numerical single phase model that includes the three-dimensional solution to the Navier–Stokes equations for a straight flow channel PEMFC, this work is the first 3D model to discuss how the mass consumed in the electrochemical reaction affects the momentum transport equations. Later they [6] used the same model to predict velocity distribution, and mass flow between channels for a serpentine flow path PEMFC. Um and Wang [7,8] developed a transient multi-dimensional model that simultaneously accounts for electrochemical kinetics, current density distribution, fluid dynamics and multi-component transport to study hydrogen dilution effects. More 3D models and solution can be found from [9–16]. However, the three-dimensional simulation for an air-breathing PEMFC is hardly found from all available literatures.

The objective of this study is to develop a three-dimensional model to account for the effect of flow dynamic, heat/mass transport and electrode kinetics on the performance of an air-breathing PEMFC. The results from this model are used to optimize the channel configuration.

2. Model descriptions

The air-breathing PEMFC model presented here is a comprehensive three-dimensional, non-isothermal, steady-state model with full mass, momentum, energy conservation governing equations. The conjugate heat transfer, species concentration solution, heat convection and conduction in solid plate, convection and diffusion in porous media electrode, and water transport through membrane are also taken into account.

2.1. Model assumptions

A complete fuel cell is an extremely complex system involving fluid dynamic, heat/mass transport phenomena and electrochemical reaction feature. In order to achieve a solution of three-dimensional model of a complete cell it is necessary to do some reasonable simplifying assumptions. In this model the following assumptions are used:

(i) The water exists in the fuel cell as vapor water.
(ii) The product water generated from the electrochemical reaction is assumed to be in the form of vapor.
(iii) Ohmic heating and ohmic resistance in the collector plate and in the carbon gas diffusion layer is neglected due to high thermal conductivity and electronic conductivity.

2.2. Geometry and calculation domain

The numerical domain used here includes full single cell geometry region. In the cathode side, air is induced into the cathode channel by natural convection. It is evident that the velocity and pressure values at the inlet and exit sections are not known a priori. To overcome this dilemma of two unknown quantities, the computation domain is extended well beyond the geometrical configuration to free the boundary condition where the pressure must be equal to that of the undisturbed environment. The computation domain, except the real physical domain, is called reservoirs. The preliminary calculations have been already carried out to ensure grid independency of solution. The minimum vertical and horizontal size of the reservoirs has been estimated which ensures accuracy of the solution results with an approximation of no more than 0.001 after carefully testing of several combinations of reservoir size. The computation domain decided for this numerical work is as illuminated in Fig. 2.

2.3. Governing equations

In the gas flow field, the flow is laminar steady state. The governing equations of fluid flow represent mathematical statements of the conservation laws of physics. There are significant commonalities between the various governing equations. In order to get ready to solve these equations, a general variable ϕ can be induced to simplify the equations, the conservation equation form of all fluid flow equations can usefully be written in the following common form [17]:

$$\nabla \cdot (\varepsilon\rho\phi\vec{u}) = \nabla \cdot (\Gamma\nabla\phi) + S_\phi \quad (1)$$

This equation can be called the transport equation for property ϕ. The term in the left hand side is a convective term, the first term in the right hand is a diffusive term, and the second term is a source term which is used for hiding the terms that are

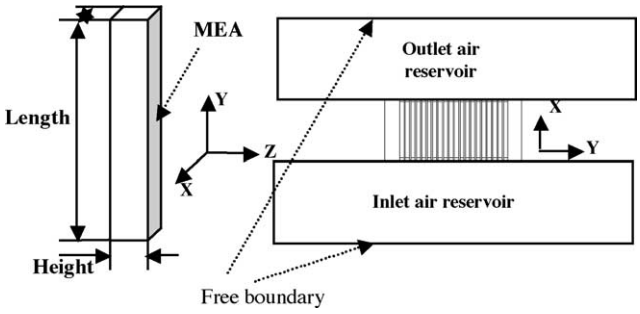

Fig. 2. Numerical simulation domain and channel dimension for an air-breathing PEMFC.

not shared and represent some source or sink of property ϕ in the control volume. The physical meaning is easy to be understood from the name of the term. We can obtain the equations of continuity, species, energy, and momentum by setting ϕ equal to 1, X_i, $\vec{u}$ and T, and selecting appropriate values for the diffusion coefficient Γ and the source term. The source terms are different for every equation in different regions, which are detailed in following parts.

2.3.1. Source term for continuity equation

In the channel and carbon diffusion layer, the source term is zero since no chemical reaction takes place there. In the anode catalyst layer, the hydrogen is consumed and the quantity of water is changed due to water transport between the anode and the cathode. The source term should equal the change of water quantity per control volume and the destruction of hydrogen:

$$S_{\mathrm{M}} = S_{\mathrm{H_2}} + S_{\mathrm{w}}^{\mathrm{a}} \tag{2}$$

where the source term for hydrogen, $S_{\mathrm{H_2}}$, can be obtained from Faraday's laws, the electrochemical reaction rate is the current density, then:

$$S_{\mathrm{H_2}} = -IM_{\mathrm{H_2}}A_{\mathrm{CV}}/2F \tag{3}$$

where A_{CV} is the specific surface area of the control volume, which is used to change the unit of the source term to become the quantity per volume. The water source in the anode side depends on the mass flow in and out of the membrane:

$$S_{\mathrm{w}}^{\mathrm{a}} = -M_{\mathrm{w}}A_{\mathrm{CV}}\alpha I/F \tag{4}$$

Analogously, in the cathode catalyst layer, the oxygen is consumed and water is produced and transported to or from anode. Thus the cathode source term is

$$S_{\mathrm{M}}^{\mathrm{c}} = -IM_{\mathrm{O_2}}A_{\mathrm{CV}}/4F + IM_{\mathrm{w}}A_{\mathrm{CV}}/2F + \alpha IM_{\mathrm{w}}A_{\mathrm{CV}}/F \tag{5}$$

The first term is the oxygen source $S_{\mathrm{O_2}}$ due to the electrochemical reaction, the second term is the water generation from the electrochemical reaction, and the third is water transport from or to the anode side. The sum of the second and the third term is water source $S_{\mathrm{w}}^{\mathrm{c}}$.

2.3.2. Source terms for momentum conservation

Source term $S_{\vec{u}}$ represents the sum of body and other external forces. In the anode channel, there is not any external force considered, so the momentum source term is zero. But in the cathode channel, the air is induced into the channel by buoyancy. The source term can be expressed in the following form:

$$S_{\vec{u}} = -\rho g \tag{6}$$

The momentum equation and the energy equation are coupled via an equation of state of ideal mixtures:

$$\rho = P/RT\left(\sum X_i/M_i\right) \tag{7}$$

In the porous medium including the carbon paper and the catalyst layers in the anode and the cathode, the source term comes from pressure drop due to the small permeability of the porous medium. Based on Darcy's law that revealed proportionality between flow rate and the applied pressure difference:

$$\vec{u} = -k_{\mathrm{P}}\nabla P/\mu \tag{8}$$

The source term in the porous medium can be expressed as:

$$S_{\vec{u}} = -\mu\vec{u}/k_{\mathrm{P}} \tag{9}$$

where k_{P} is the permeability of the medium, which is independent of the nature of the fluid but depends on the geometry of the medium.

2.3.3. Source term for energy conservation

Energy source term S_{T} represents the rate of increase of energy due to heat sources or sinks. In the catalyst layer, because of the heat transformed from the irreversible overpotential, the source term is:

$$S_{\mathrm{T}}^{\mathrm{a}} = I\eta_{\mathrm{a}}, \qquad S_{\mathrm{T}}^{\mathrm{c}} = I\eta_{\mathrm{c}} \tag{10}$$

In the membrane, the heat is generated from ohmic resistance, so

$$S_{\mathrm{T}}^{\mathrm{m}} = I\eta_{\mathrm{m}} \tag{11}$$

2.3.4. Water transport in membrane

For the air-breathing PEMFCs that operate in a dry anode gas to reduce the size of the fuel cell system, a certain amount of product water transports from the cathode to the anode due to concentration difference, which is actually called back diffusion. When current is drawn from the cell, protons migrate from the anode to the cathode and carry with them water molecules and this process is called electro-osmotic drag. Hence, the amount of water collected at the anode is equal to the difference between the amount of water back diffusion and the water transported by osmotic drag.

Based on the assumption that the gradient of water concentration across the membrane can be approximated by a single-step linear difference between the concentration in the cathode and anode, the final expression net water molecular per proton flux can be yielded as:

$$\alpha = n_{\mathrm{d}} - FD_{\mathrm{w}}(C_{\mathrm{w,c}} - C_{\mathrm{w,a}})/It_{\mathrm{m}} \tag{12}$$

where the diffusion coefficient, and electro-osmotic coefficient can be calculated as a function of water content in a membrane based on the correlations by Springer et al. [18]:

$$n_{\mathrm{d}} = 0.0029\lambda^2 + 0.05\lambda - 3.4 \times 10^{-19} \tag{13}$$

$$D_{\mathrm{w}} = D_\lambda \exp(2416((1/T_0) - (1/T))), \quad T_0 = 303\,\mathrm{K} \tag{14}$$

where

$$D_\lambda = 10^{-6}, \quad \lambda < 2 \tag{15}$$

Table 1
Values for parameters and boundary condition used in the model

Parameters	Symbol	Value
Porosity in carbon paper and catalyst layer	ε	0.4, 0.28
Average current density	I_{avg}	0.15 A cm^{-2}
Ambient temperature, pressure	T_b, P	299 K, 101325 Pa
Anode channel width, height	w_a, h_a	0.1 cm
H_2 inlet temperature	T_a	299 K
H_2 flow rate in inlet	N_{H_2}	7.198E−08 kg s^{-1}
Permeability in GDL	k_P	1.8E−18 m^2
Permeability in catalyst layer	k_P	1.76E−12 m^2
Cathode channel height and width	h_c, w_c	0.3 cm
Relative humidity in air	ξ	63% RH
Membrane dry density	ρ_{dry}	1840 kg m^{-3}
Membrane dry equivalent weight	M_{dry}	1100 kg kmol^{-1}
Membrane thickness	t_m	0.00508 cm
Thickness of diffusion layer, catalyst layer	t_d, t_s	0.026 cm, 0.001 cm
Oxygen/nitrogen ratio in air	ζ	0.21/0.79
Cathode channel length	L_c	49 mm

$$D_\lambda = 10^{-6}(1 + 2(\lambda - 2)), \quad 2 \le \lambda \le 3 \tag{16}$$

$$D_\lambda = 10^{-6}(3 - 1.67(\lambda - 3)), \quad 3 < \lambda \le 4.5 \tag{17}$$

$$D_\lambda = 1.25 \times 10^{-6}, \quad \lambda \ge 4.5 \tag{18}$$

$$C_w, C_{w,a} = (\rho_{dry}/m_{dry})\lambda \tag{19}$$

The water content λ in the membrane is given as a function of the activity of water by expression:

$$\lambda = 0.043 + 17.8a - 39.85a^2 + 36a^3, \quad 0 \le a \le 1 \tag{20}$$

$$\lambda = 14 + 1.4(a - 1), \quad 1 < a \le 3 \tag{21}$$

where the water activity a is given by

$$a = P_w / P_w^{sat} \tag{22}$$

P_w^{sat} is the saturation vapor pressure of water at 'k' interface and calculation equation of it is given by [18].

2.3.5. Electrochemical equations

In this model, activity over-potential, proton transport resistance in membrane and oxygen transport limitation are involved in the voltage losses. The detailed equations are:

$$V_C = V_{OC} - \eta_{act} - \eta_{ohm} - \eta_{conc} \tag{23}$$

$$\eta_{act} = (RT/0.5F)\ \ln(I/I^0 P_{O_2}) \tag{24}$$

$$\eta_{ohm} = t_m I/\sigma_m \tag{25}$$

$$\eta_{conc} = -\mathrm{BT}\ln(1 - I/I_{lim}) \tag{26}$$

The membrane conductivity, σ_m, can be calculated as a function of the water content.

$$\sigma_m = (0.00514\lambda - 0.0326)\exp[1268((1/303) - (1/T_m))] \tag{27}$$

The concentration losses are related to oxygen mass transfer rate. The mass transfer rate is generally characterized by a mass transfer coefficient h_m, which is the rate of mass transport due to convection and diffusion. For oxygen transport it can be written as:

$$\dot{m}_{O_2} = h_M^{O_2} \rho_{mix}(X_{O_2}^\infty - X_{O_2}) \tag{28}$$

The dimensionless mass transfer coefficient Sherwood number is calculated by:

$$Sh = h_M^{O_2} L/D_{O_2} \tag{29}$$

Then the limited current density equation becomes [19]:

$$I_{lim} = 4FD_{O_2}C_{O_2}^\infty\, Sh/L \tag{30}$$

2.4. Boundary and initial conditions

The anode inlet velocity can be calculated from the flow rate, which depends on stoichiometry. The exit of the anode side assumes ambient pressure to be the boundary condition. In the cathode side, the boundary conditions both in the inlet and outlet are free pressure condition after adding enough reservoir. The heat resistance between the different regions in the cell is not taken into account. The hydrogen flow rate in the anode inlet, and the parameters used in the model can be found in Table 1.

2.5. Solution strategy

The model was solved based on SIMPLE algorithm and MARS (monotone advection and reconstruction scheme). The process was executed in the commercial flow dynamic software STAR-CD V3150 for the Linux operation system. The finite control volume technique was used for solving the problem. The governing equations for electrochemical reactions in the MEA and water transport in the membrane were solved simultaneously by a user subroutine in the form of FORTRAN code based on the finite differential approach. The source terms for the governing equations were incorporated into STAR-CD through the introduction of a user subroutine. Results were checked for convergence.

3. Results and discussion

3.1. Model validation

To validate the numerical model presented in the preceding section, an experiment has been carried out in our laboratory for the same single cell operating at a specified operation condition using a fuel cell test facility Hewlett Packard 34970A Data Acquisition/Switch unit. Dry hydrogen having purity of 99.99% was fed into the anode channel. The stoichiometry of 1.0 is used for the hydrogen flow rate. The air supply to the cathode was spontaneously obtained by natural convection from environmental air without external heating and humidity. The curve of voltage versus current density has been

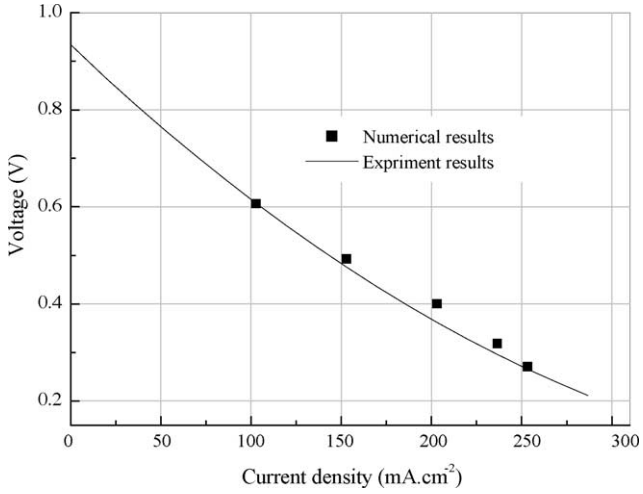

Fig. 3. Comparison between the numerical prediction and experimental results.

tested to verify the simulation result. The computed voltages for several current densities, as shown in Fig. 3, are in good agreement with the experimental data. However, the calculation current densities for the cell are a little higher than the experimental values. This discrepancy could be explained from the assumption of vapor water. Liquid water was not considered in this model, however, in the practical operation, a quantity of liquid water did appear and there was flooding in the cathode when it was operated at high current density, which resulted in the calculated voltage being a little higher than experiment results. Liquid water will be considered in the future work.

3.2. Effect of channel configuration

Based on the above model and boundary condition, simulations were performed for three cases of different channel widths, 2, 3, and 4 mm. The rib width is fixed to 1 mm in every case. Based on the following equations, the calculated open ratios corresponding to the channel width are 67.5, 75.9, 80%, and the land area fractions are, respectively, 0.4814, 0.3175, and 0.25:

$$\bar{o} = w_{\text{channel}} \times \text{int}(w_{\text{total}}/(w_{\text{channel}} + w_{\text{rib}}))/w_{\text{total}} \quad (31)$$

$$\iota = (1 - \bar{o})/\bar{o} \quad (32)$$

The anode channel and configuration is fixed for the discussion of the cathode channel effect on the cell performance. The cathode channel height is fixed to 3 mm and the length is 49 mm. The electrode area is 34 cm^2. Some results obtained from calculation at a current density of 150 mA cm^{-2} are presented here to investigate the effect of cathode channel configuration on mass transfer and water management, and on the performance of an air-breathing PEMFC.

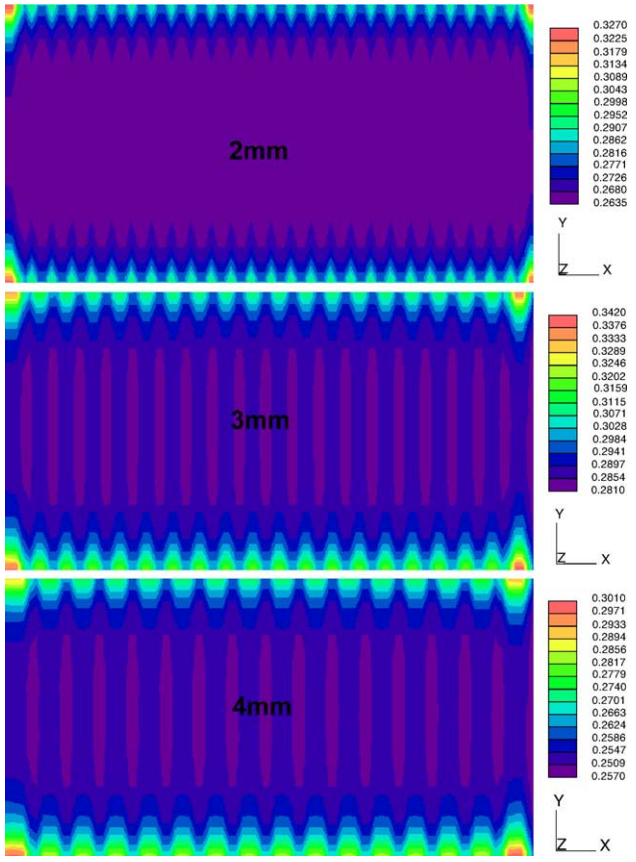

Fig. 4. Comparison of limiting current density distribution (A cm^{-2}).

3.2.1. Mass transfer

Fig. 4 shows a detailed distribution of the limiting current density for three channel widths. The calculated average limiting current densities from Fig. 4 are, respectively, 0.268, 0.279 and 0.255 A cm^{-2} for the cells with 2, 3 and 4 mm air channels. It shows that the average limiting current density is the highest when the channel width is 3 mm. That means the cell with 3 mm channel is better for oxygen transportation. This can be explained as follows. When air with some velocity is induced into the channel, in the entrance region, the velocity boundary layer has not developed, where the sufficient variation in velocity and temperature takes place near the wall. Heat and mass transfer are thus enforced. It is known that the smaller the width is, the smaller the entrance length is, and then the flow is fully developed sooner. Therefore, from this point of view, the bigger channel width that has a longer entrance is beneficial for sufficient heat and mass transfer. In addition, in the laminar flow, the flow resistance in a channel is inversely proportional to the channel width when the channel depth is fixed. Therefore, the bigger channel with the lower flow resistance also induces air flowing into the cathode channel more easily. However, if the channel width is too big then the flow and the mass/heat transfer are also limited by the thermal boundary layer effect. Because the two thermal boundary layers in the side wall are distinct from each

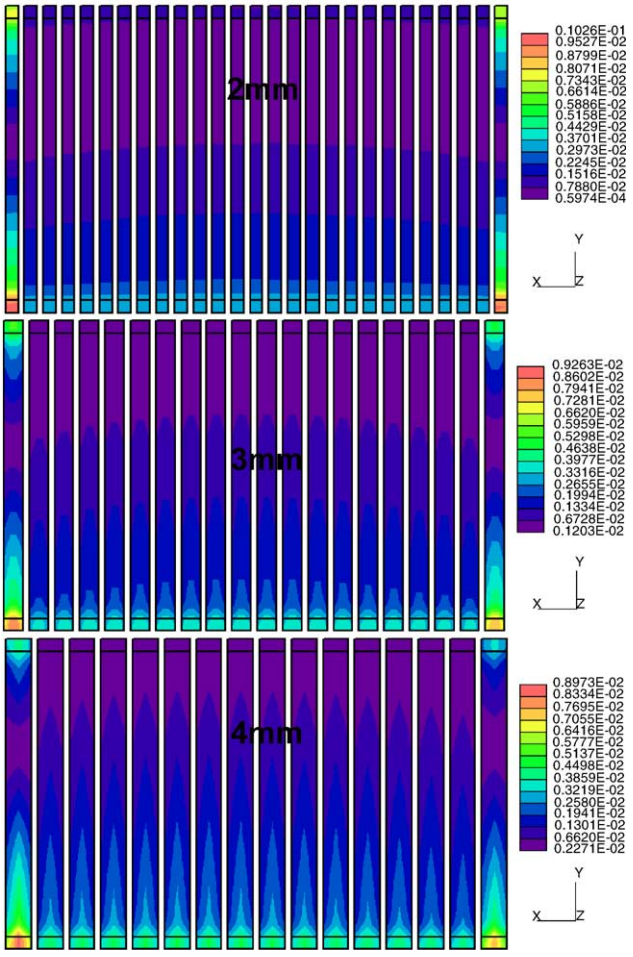

Fig. 5. Comparison of velocity profile in cathode channel ($m\,s^{-1}$).

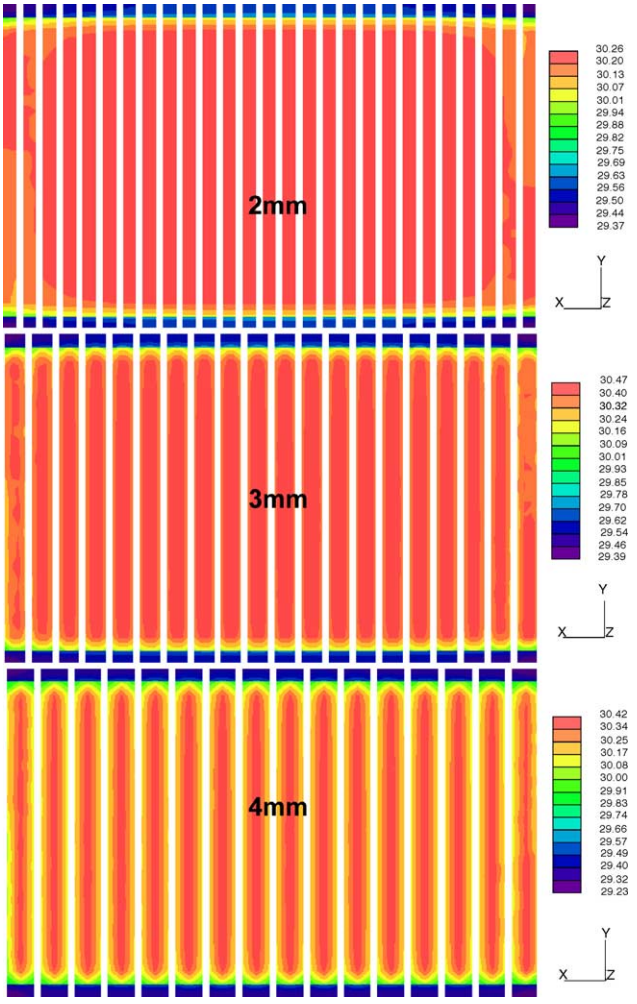

Fig. 6. Comparison of temperature distribution in cathode channel (°C).

other, they cannot affect the free stream in the center sufficiently. Thus natural convection is also weakened. This can be proved from Figs. 5 and 6. Fig. 5 shows the velocity profile in the cathode channel for three different channel widths. The 4 mm channel has the longest entrance length. Fig. 6 shows the temperature profile in the cathode channel. It shows the temperature boundary effect. In the 2 mm channel, the thermal boundary layer is scarcely visible, thus the heat transfer to the side wall is strong, which can also be obtained by a large land area fraction. Strong heat transfer to the side wall is not always good for heat transfer to the gas region. On the contrary, the 4 mm channel has two distinct thermal boundary layers. The temperature in the channel cannot remain high due to the large volume of the gas region. Fig. 7 shows the temperature distribution in the catalyst layer for three channel widths. It shows that the temperature of the cathode catalyst layer for the 3 mm channel is the highest. The reason has already been accounted for above. Fig. 8 shows the distribution of the concentration losses due to oxygen transport limitation. The average concentration over-potentials are, respectively, 0.106, 0.0952 and 0.117 V for the three channel widths from 2 to 4 mm. The highest oxygen concentration losses can be observed in the 4 mm channel. The 3 mm channel has the best oxygen mass transport effect. It also can be seen that in the left and right area which, under the cathode channel and near the hydrogen inlet and outlet, has the strongest mass transfer due to the effect of anode water and hydrogen distribution. In the area near the intake of the cathode channel, the mass transfer also is stronger. Hence the higher temperature can also be observed in these regions.

3.2.2. Water transportation in the membrane

Because the air-breathing PEMFC works on dry anode gas, the sources of water in the anode are only the product in the cathode and the humidity in air. If back diffusion cannot supply enough water to the anode side, the membrane in the anode side is dehydrated. Then the ohmic losses in the membrane will affect the performance of the cell due to low proton conductivity. Fig. 9 shows the distribution of the water mass fraction at the anode catalyst layer for various channel widths of 2, 3 and 4 mm, respectively. It is observed that the back-transport of water at the anode is dependent on

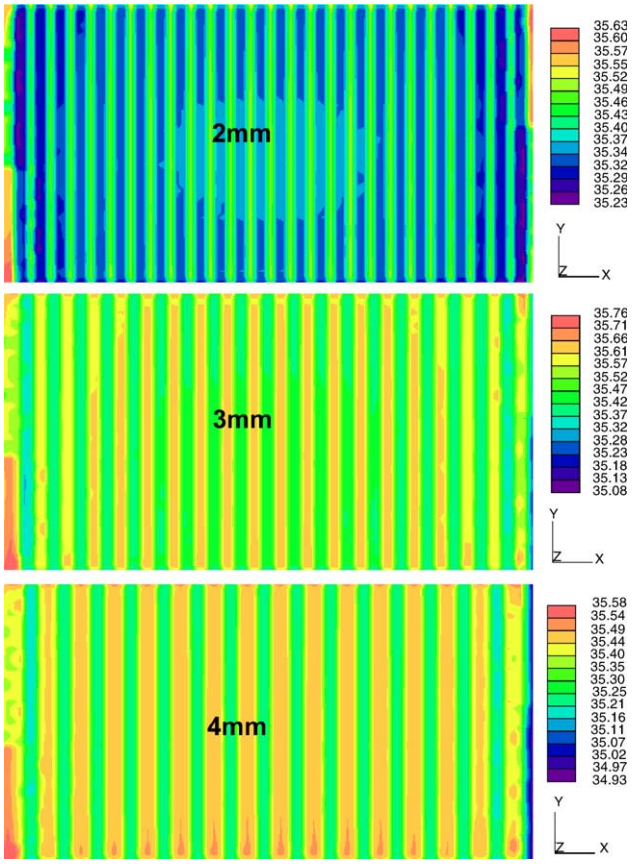

Fig. 7. Comparison of temperature distribution in cathode catalyst layer (°C).

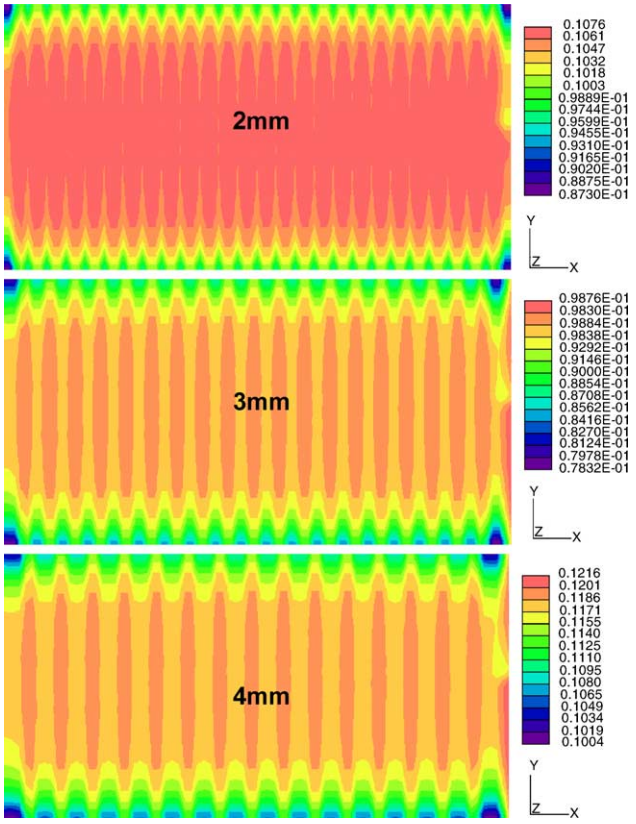

Fig. 8. Comparison of concentration losses profile (V).

both the current density and the water concentration gradient across the membrane. In the region near the air intake and vent where the current density is high, the anode water concentration is low because much water is carried by protons to the cathode. In the center, where the current density is low, the water concentration is high due to a strong back diffusion taking place. In the anode inlet region the water concentration is the lowest because pure hydrogen is used as anode reactant. It also clearly shows that water transport in the membrane is affected by the flow field design. In this base case, a bigger channel has a better water back diffusion; the 4 mm channel has the best membrane hydration in the anode side. Fig. 10 shows the distribution of net water per proton mole flux ratio. It shows that the osmotic drag takes place wherever there is more proton transport (high current density region), and in other regions, back diffusion takes place. Different flow fields result in different water transport characters. In this air-breathing PEMFC without external humidity case, the stronger back diffusion is obtained from the larger real value of net water transport, however, if comparing the absolute value, then the small value of that means strong back diffusion. Fig. 11 shows distribution voltage losses due to membrane ohmic resistance for three cases; it shows that the membrane was better hydrated when the bigger channel width is used, and then, the ohmic losses in the membrane are

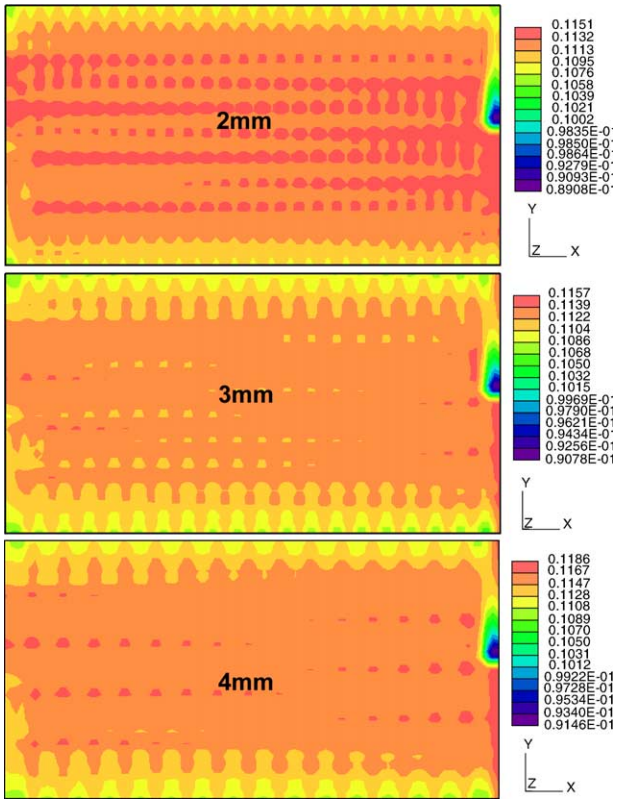

Fig. 9. Comparison of water mass fraction distribution in anode catalyst layer.

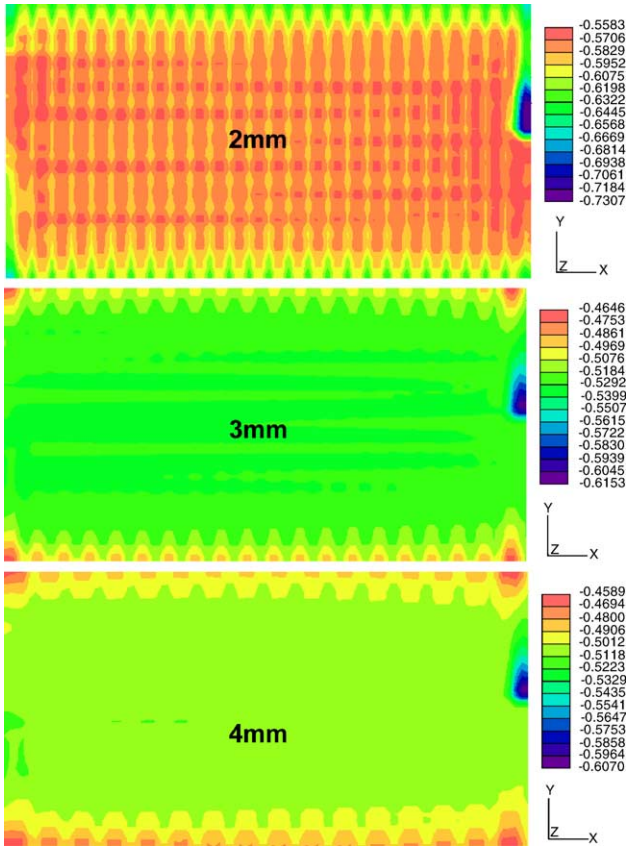

Fig. 10. Comparison of net water transport rate through membrane.

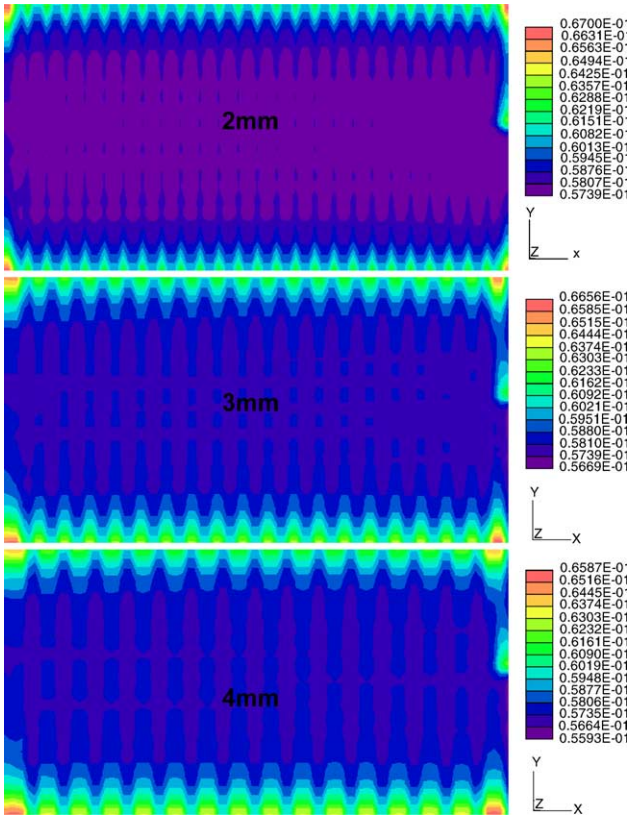

Fig. 11. Comparison of ohmic losses distribution in membrane (V).

decreased. It can be explained as follows. The back diffusion mostly depends on water concentration difference between the cathode and the anode sides. When the channel width increases, the open ratio is also increased and thus more MEA area is under the cathode channel where the water concentration is high due to the electrochemical reaction. On the other hand, in the anode side the water concentration is zero at first for every case. Hence the bigger water concentration is come into being for the large open ratio, and thus the back diffusion is enforced and membrane hydration is improved.

3.2.3. *The performance of cell*

Fig. 12 shows polarization curves for three cases. The voltage is calculated from several different current densities. It shows the cell with the channel width of 3 mm has the best performance in this case. Considering the above discussion it can be understood easily. The most important rule for optimization of the channel configuration in air-breathing PEMFCs is the consideration of mass/heat transfer and water transport through the membrane. Good channel configuration should benefit mass transfer and water back diffusion. However, some deficiencies in this calculation should be taken into account in the next work. From Fig. 12, it can be observed that the downward slope decreases between current densities of 150 and 200 mA cm^{-2} before mass transport over-potential takes place. This anomaly is because liquid water was not considered in this model. Thus the performance was calculated to be increased at high current density where liquid water appears and blocking the gas way in practical operation. Additionally, in practice, there are other performance losses such as ohmic losses in other components of bipolar plate and diffusion layer, and contact resistance. These losses also affect the cell performance especially the contact resistance which plays a great role on performance losses. If the

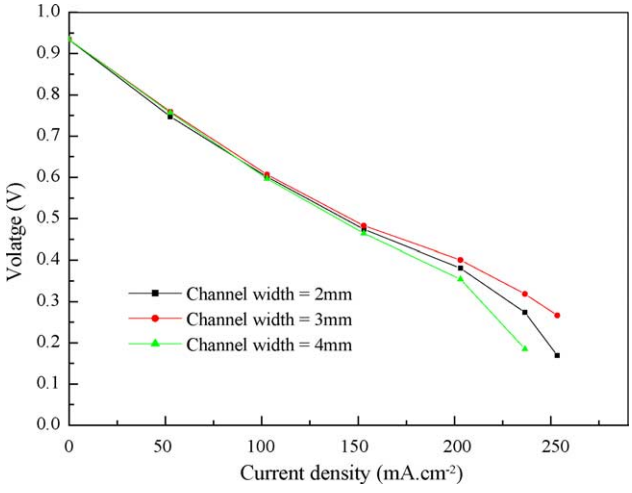

Fig. 12. Performance curves for three channel width.

land fraction is too small, the contact resistance ohmic losses should be considered for channel design.

4. Conclusions

A three-dimensional comprehensive model has been developed. The model fits the experimental data well for any reasonable working current density. Using the model, the effects of channel size on the concentration losses and water transport in the membrane have been obtained numerically. The model provides an insight into the water transfer mechanism and the onset of mass transport limitations in air-breathing PEMFCs. When the open ratio of the channel is too small, velocity in the channel cannot be developed sufficiently, and the heat transfer in the gas area is reduced due to more heat transfer to the solid land. Hence the natural convection cannot be strong. On the contrary, when the open ratio of the channel is too big, heat transfer is also greatly weakened by the large volume of gas area and the thermal boundary effect. Natural convection also cannot be enforced. Comparing the three channel width when rib size and height is fixed, the 3 mm channel width can achieve the best performance in this base case. For the case of water transfer in the membrane, the wide channel can strengthen back diffusion in this operation condition. Also if the width of the channel is too big, the contact resistance must be increased sufficiently. The good performance gained from improved membrane proton conductivity is diminished by the contact resistance for electrons. Therefore, in air-breathing PEMFCs designs, the many trade-off should be considered to obtain high mass transfer for oxygen, better humidity in the membrane, and a lower contact resistance. This model is demonstrated to be used as a tool for the optimization of air-breathing PEMFCs.

References

[1] C.Y. Chen, P. Yang, J. Power Sources 123 (1) (2003) 37–42.
[2] D. Chu, R. Jiang, J. Power Sources 83 (1999) 128–133.
[3] P.-W. Li, T. Zhang, Q.-M. Wang, L. Schaefer, M.K. Chyu, J. Power Sources 114 (2003) 63–69.
[4] T. Hottinen, M. Mikkola, P. Lund, J. Power Sources 129 (1) (2004) 68–72.
[5] S. Dutta, S. Shimpalee, J.W. Van Zee, J. Appl. Electrochem. 30 (2000) 135–146.
[6] S. Dutta, S. Shimpalee, J.W. Van Zee, Int. J. Heat Mass Transfer 44 (2001) 2029–2042.
[7] S. Um, C.Y. Wang, J. Electrochem. Soc. 147 (12) (2000) 4485–4493.
[8] S. Um, C.Y. Wang, Proceedings of the ASME Fuel Cell Division, The 2000 ASME IMECE, Walt Disney World Dolphin, Orlando, Fl, November 5–10, 2000.
[9] T.-C. Jen, T. Yan, S.-H. Chan, Int. J. Heat Mass Transfer 46 (2003) 4157–4168.
[10] D. Natarajan, T. Van Nguyen, J. Power Sources 115 (2003) 66–80.
[11] P.-W. Li, L. Schaefer, Q.-M. Wang, T. Zhang, M.K. Chyu, J. Power Sources 115 (2003) 90–100.
[12] T. Berning, D.M. Lu, N. Djilali, J. Power Sources 106 (2002) 284–294.
[13] A.S. Kheireddine, M. Hpoula Sanda, S.K. Cheturvedi, T.O. Mohieidin, Energy 22 (4) (1997) 413–423.
[14] K.P. Recknagle, R.E. Williford, L.A. Chick, D.R. Reactor, M.A. Khaleel, J. Power Sources 113 (2003) 109–114.
[15] M. Hu, A. Gu, M. Wang, X. Zhu, L. Yu, Energy Convers. Manage. 45 (2004) 1861–1882.
[16] G. Hu, J. Fan, S. Chen, Y. Liu, K. Cen, J. Power Sources (2004).
[17] H.K. Versteeg, W. Malalasekera, An Introduction to Computational Fluid Dynamics, Longman, 1995.
[18] T.E. Springer, T.A. Zawodzinski, S. Gottesfeld, J. Electrochem. Soc. 138 (8) (1991) 2334–2341.
[19] G. Prentice, Electrochemical Engineering Principles, Prentice-Hall, 1991.